The potential scarcity, or not, of polymeric overall water splitting photocatalysts

Benedict Saunders,[1,2] Liam Wilbraham,[1,3] Andrew W. Prentice,[1] Reiner Sebastian Sprick,[4] Martijn A. Zwijnenburg[1,*]
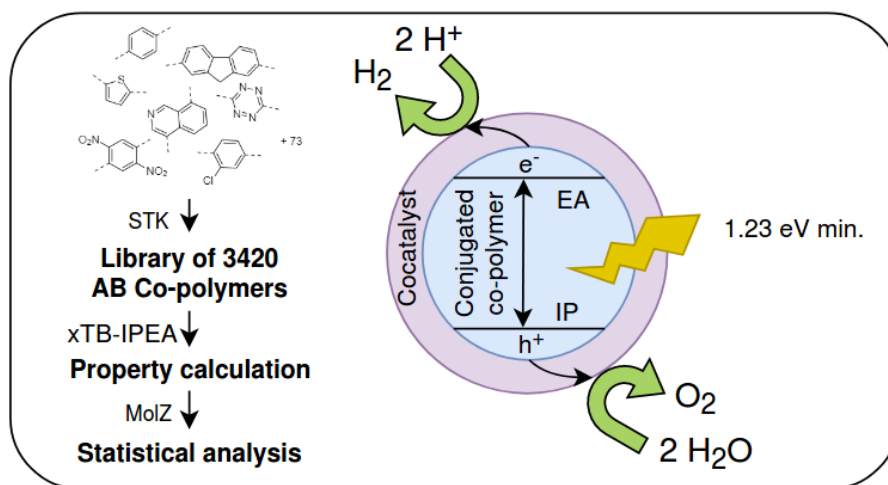
[1] Department of Chemistry, University College London, 20 Gordon Street, London WC1H 0AJ, U.K.

[2] Currently at the Department of Chemistry, University of Warwick, Coventry CV4 7SH, U.K.

[3] Currently at Exscientia, Oxford Science Park, Oxford, OX4 4GE, U.K.

[4] Department of Pure and Applied Chemistry, University of Strathclyde, 295 Cathedral Street, Glasgow, G1 1XL, U.K.

[*]Email: m.zwijnenburg@ucl.ac.uk

We perform a high-throughput virtual screening of a set of 3240 conjugated alternating binary co-polymers and homo-polymers, in which we predict their ability to drive sacrificial hydrogen evolution and overall water splitting when illuminated with visible light. We use the outcome of this screening to analyse how common the ability to drive either reaction is for conjugated polymers loaded with suitable co-catalysts, and to suggest promising (co-)monomers for polymeric overall water splitting catalysts.

Introduction

In recent years organic materials, particularly conjugated polymers, have come to the foreground as potential photocatalysts for splitting water into molecular hydrogen and oxygen.[1-5] The hydrogen produced in this way would be renewable and green, emitting nothing but water upon combustion, making it a viable candidate for a sustainable replacement for current carbonaceous fuels. While more than a hundred polymers and other organic materials are known to be experimentally active for photocatalytic hydrogen evolution when studied in the presence of a metal co-catalyst and a sacrificial electron donor (SED),[2, 6-7] a much smaller number has been observed to oxidise water in the presence of a co-catalyst and a sacrificial electron acceptor (SEA),[8-11] and a smaller number still with the ability to drive overall water splitting when illuminated by solar light.[2, 12-16] Examples of the latter include carbon nitride[12-13, 16] and covalent triazine-based framework materials.[14-15] Here, we computationally screen a very large dataset of organic (co-)polymers to understand if this apparent experimental scarcity of organic materials that, under illumination with visible light, can oxidise water and drive the overall splitting of water is due to thermodynamic constraints inherent to the material class or is kinetic in nature. In the latter case materials that appear inactive could potentially become active in the presence of the right co-catalyst(s) or when part of a heterojunction, accelerating otherwise sluggish water oxidation kinetics and/or minimising undesired electron-hole recombination.

From a thermodynamic perspective, for a material to reduce protons and oxidise water when illuminated, the material's ionisation potential (IP, valence band maximum) and electron affinity (EA, conduction band minimum) should at least straddle the solution proton reduction and water oxidation potentials, the latter defined – as is convention – in terms of the potential of the equivalent reduction reaction (see figure 1a). Similarly, to reduce protons and oxidise a SED or oxidise water and reduce a SEA the material's IP and EA should straddle the proton reduction and SED oxidation or the SEA reduction and water oxidation potentials, respectively, once again defining the oxidation potentials in terms of that of the equivalent reduction half-reactions. It is highly desirable not only for the material to be active, but to be active under visible light, as most of the sunlight is concentrated in this part of the spectrum. Therefore,

the material's optical gap, the energy below and wavelength above which the material is transparent to light, needs to be as small as possible. However, at the same time the materials' optical gap needs to be larger than the difference between the potentials of the relevant solution reduction and oxidation half-reactions, 1.23 (e)V in the case of overall water splitting. Otherwise, the photons would not deliver enough energy for the relevant overall reaction to be thermodynamically favourable. The fact that the exciton binding energy in organic materials, even after immersion in water, is not negligible and that the excitons, excited electron-hole pairs, formed initially by the absorption of light do not spontaneously dissociate into free electrons and holes complicates the above picture slightly.[17] Conceptually, in the case of materials with a non-negligible exciton binding energy we need to consider besides IP and EA also IP* and EA*, the ionisation potential and electron affinity of the excitons, respectively.[18-19] However, in practice when screening materials the effect of the missing exciton binding energy, typically 0.1–0.2 (e)V[17] can be absorbed in a requirement for a similar overpotential on top of the thermodynamic solution potentials. Other properties than a material's IP, EA and optical gap, such as its wettability and dispersibility in water or its particle size distribution, will clearly influence its photocatalytic activity. However, if a material is thermodynamically unable to oxidise water or reduce protons, or doesn't absorb sun light, it simply won't act as a water splitting photocatalyst, irrespective of how well it's wetted by or disperses in water or how big or small the particles are. This binary quality of IP, EA and the optical gap, makes them key parameters to screen when trying to understand how common the ability to photocatalytically split water is in a class of materials such as conjugated polymers.

Previous work by our group demonstrated that density functional theory (DFT) can accurately predict the IP and EA values of conjugated polymers when compared to experimental photoelectron spectroscopy[20-21] and that these DFT predicted IP and EA values can be successfully used to explain the trends in the activity of such polymers for sacrificial hydrogen evolution.[7, 22-25] However, calculating the IP and EA, as well as optical gap of thousands of polymers, with DFT and its time-dependent extension (TD-DFT) would be prohibitively computationally expensive. However, we demonstrated previously that calculations using the xTB family of tight-binding DFT methods,[26]

developed by Grimme and co-workers, after calibration to (TD-)DFT results give very similar results for a fraction of the computational cost[27] and allow for the convenient calculation of properties such as IP, EA and optical gap, of tens of thousands molecules and/or polymers.[6, 28-30] The xTB calculations, GFN1-xTB[31] for ground-state geometries, IPEA-xTB[32] for IP and EA, and sTDA-xTB[33] for the optical gap, are performed on a single polymer chain, embedded in the case of GFN1-xTB and IPEA-xTB in a dielectric continuum with the relative dielectric permittivity of water. In previous work, it was shown that use of such a minimal model of a polymer in DFT calculation gives a good fit to experimentally measured IP and EA values for dry polymer solids.[20-21] Using calibrated xTB we predict the IP, EA and optical gap values of a dataset consisting of 3240 conjugated alternating binary co-polymers and homo-polymers built from a library of 80 monomers, see figures 1b and 1c, and analyse what fraction of the dataset can evolve hydrogen in the presence of a commonly used SED, triethylamine (TEA), and what fraction of polymers can drive the overall splitting of water. We discuss how these numbers change when we require the polymer to work using visible light and, finally, present the monomers which are overrepresented in the polymers that are active in the visible. Such monomers would make good candidates to explore experimentally when synthesising polymer photocatalysts.

Methodology

We assembled 3240 oligomers from all possible binary AB combinations of the library of 80 monomers, including 80 homo-oligomers (see figures 1b). A selection of the monomers is shown in figure 1C; the full library is displayed in figure S1 in the supporting information. For each oligomer, a SMILES representation was generated using the stk[34-35] python package, such that each oligomer contained 16 individual monomers (8 -AB- repeat units for the alternating co-polymers, 16 -A- repeat units for the homo-polymers). As SMILES strings contain no explicit geometry information, a subsequent conformer search was required which we performed using the ETKDG[36] algorithm as implemented in *RDKit,[37]* a cheminformatics library, generating 500 conformers for each oligomer and optimising each with the MMFF94[38] forcefield. The conformer with the lowest forcefield energy was selected and optimised further with

GFN1-xTB,[31] as implemented in xtb 5.6.4SE,[39] in preparation for the calculation of IP, EA and optical gap.
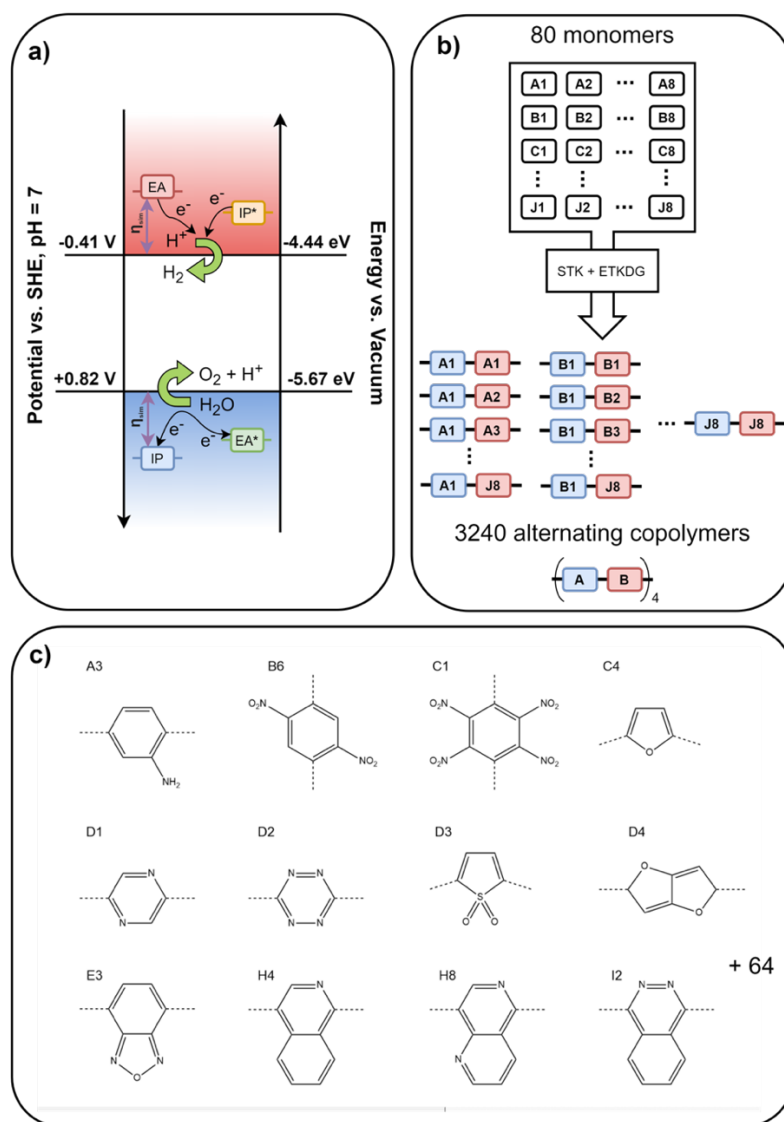

Fig. 1 *(a) Schematic illustration of the alignment of IP and EA, and their excited state counterparts IP* and EA*, relative to the potentials for proton reduction and water oxidation required for overall water splitting, (b) Oligomer assembly methodology, (c) Subset of the 80 monomers studied herein (all 80 monomers are shown in figure S1 in the supplementary information).*

The IPEA-xTB[31] variant of xTB was used to predict the vertical IP and EA values of the oligomer, with solvation in water represented by the generalised Born surface area (GBSA) model.[40] The singlet excitation spectra of the oligomers were calculated with

the sTDA-xTB[33] method, the lowest of which was taken to be the optical gap. The sTDA-xTB calculations do not include solvation as that is not implemented for sTDA-xTB. The GFN1/IPEA/sTDA-xTB predicted IP, EA and optical gap values for each oligomer were then transformed to values that can be directly compared to previous (TD-)DFT predictions through a linear scaling model, calibrated in prior work by us[27] to (TD-)DFT results for oligomers immersed in water. An independent linear model was used for each of the three properties, see Table S1 for the model parameters used. The mean average deviation (MAD) of these models based on the initial training set were 0.08, 0.06 and 0.13 (e)V for IP/EA/optical gap respectively, increasing to 0.16/0.14/0.16 (e)V for a validation set of polymers not included in the training set. These MAD values are reasonable such that the calibration should be transferrable to the wide range of polymers considered herein.

A locally adapted version of the *MolZ* python package[41] allows us to query our dataset and assign a z-score to each of the 80 monomers, which provides an insight into the contribution of each monomer to the queried properties. To calculate the z-score we describe the statistics of the scenario where we have a dataset of N polymers, k of which contain a particular monomer i, and n polymers in a sub-set of the dataset with desirable properties, p of which contain i, in terms of a hypergeometric distribution with a mean ($\bar{x}$) and variance (σ^2) of:

$$\bar{x} = \frac{nk}{N}$$

$$\sigma^2 = \frac{nk(N-k)(N-n)}{N^2(N-1)}.$$

From the mean and variance of the distribution we can then calculate the z-score for a particular value of p via:

$$\text{z-score}_i = \frac{(p-\bar{x})}{\sigma^2}.$$

Large positive z-scores indicate that monomer i is overrepresented in the sub-set of polymers relative to other monomers and hence likely a good monomer choice for achieving the properties representative of that subset.

Results and Discussion

First, we analyse what fraction of the 3240 polymers can evolve hydrogen in the presence of TEA as the SED. As can be seen from figure 2a more than 95% of the polymers in the dataset, even if limiting ourselves to polymers with an absorption onset in the visible region (figure 2b), can thermodynamically drive the reduction of protons and the 2-electron oxidation of TEA to diethylamine and acetaldehyde at pH 12.3 (-0.76 V). The latter is the experimentally determined pH of the mixture of TEA, water and methanol used in photocatalysis experiments.[42] The percentage of polymers able to drive both half-reactions decreases steadily when we require an additional overpotential for both of the two half-reactions. Still, for an overpotential value of 0.3 V, proton reduction and 2-electron oxidation of TEA is predicted to be favourable for more than 80% of the dataset.

Proton reduction and hydrogen-hydrogen bond formation is typically catalysed by added platinum nanoparticles or palladium nanoparticles remaining from the catalyst used in polymer synthesis.[43-44] Polymers can also potentially act as a catalyst for proton reduction themselves but in the presence of palladium or platinum nanoparticles the activity of those will very likely outcompete any inherent catalytic activity of the polymer.[45] In contrast, TEA oxidation most likely is not catalytic, and probably takes the form of two sequential out-of-sphere electron-transfer steps between the polymer and TEA. First TEA gets oxidised to TEA$^+$, which after deprotonation, gets oxidised in the second electron-transfer step to diethylamine and acetaldehyde, the expected 2-electron oxidation products. To efficiently oxidise TEA a polymer's IP should thus probably not only be more positive than the potential of the half-reaction associated with the 2-electron oxidation of TEA but also be more positive than that for the 1-electron oxidation of TEA (0.64 V at pH 12.3), as otherwise the 1-electron oxidation step might act as a thermodynamic barrier.[24] Indeed, we observed in previous combined computational and experimental studies that polymers which are experimentally highly active for sacrificial hydrogen evolution in the presence of TEA have such predicted positive IP values.[7, 23-25, 27]
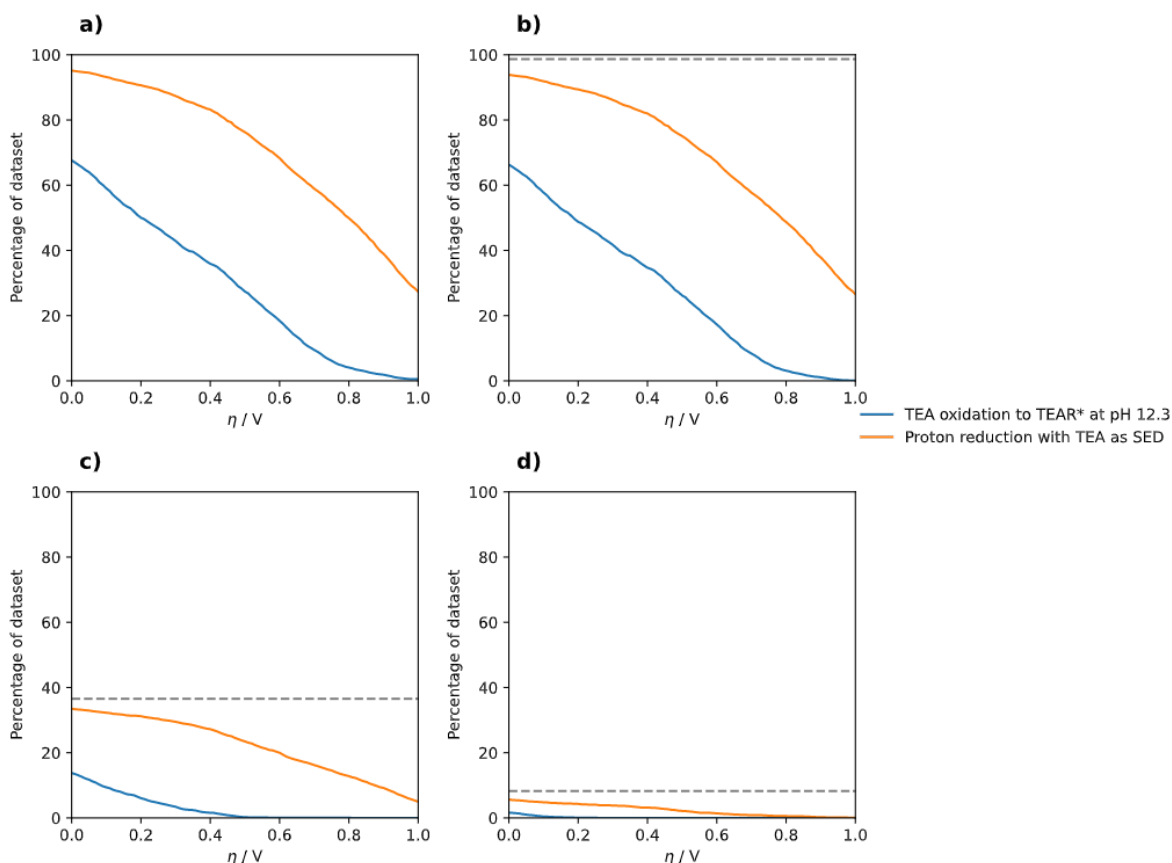
Fig. 2 *Percentage of (co-)polymers in the dataset that are predicted to be able to drive the reduction of protons and the overall oxidation of TEA (orange line) and the one-hole oxidation of TEA (blue line) at pH 12.3 for different optical gap ranges. Panel (a) does not include a limitation on the optical gap. Panel (b) introduces a limitation such that the predicted optical gap must be ≤ 3.5 eV, which is reduced to 2.5 eV in plot (c) and finally 2.0 eV in plot (d). The grey dashed lines in panels b-d indicate the number of polymers in the entire dataset that fall within each optical gap constraint. See figure S2 for a zoomed in version of a-d.*

Going back to figure 2a we can see that a smaller percentage of the dataset can drive both proton reduction and the 1-electron oxidation of TEA at pH 12.3, between 60 and 70% in the absence of an overpotential requirement and approximately 40% for an overpotential of 0.3 V. Figures 2c and 2d finally demonstrate that if we require a polymer not only be able to reduce protons and oxidise TEA but also to have an optical gap that is small enough to absorb a large part of the visible spectrum the percentages get truly small. This reduction, especially in the case when considering the 2-electron oxidation of TEA and proton reduction, is mainly the direct results of the optical gap

restriction. Of the 3240 polymers in the dataset 3197 (98.7%) have an optical gap below 3.5 eV, 1184 (36.5%) have an optical gap below 2.5 eV and only 267 (8.2%) have an optical gap below 2.0 eV (see dashed lines in figures 2b-2d). However, when considering the 1-electron oxidation of TEA and proton reduction there is a clear further reduction, which probably stems from the fact that polymers with a small optical gap also will have a small fundamental gap, the difference between IP and EA, which might straddle the potentials for the 2-electron oxidation of TEA and proton reduction but not those for the 1-electron oxidation of TEA and proton reduction.

Figure 3 shows the case of overall water splitting but now as a function of pH. For neutral water, pH 7, more than 50% of polymers are predicted to straddle the proton reduction and water oxidation potentials, which reduces to a still respectable more than 30% when requiring an additional 0.3 V overpotential for both half-reactions. This 30% includes those linear conjugated polymers that have been previously reported in the literature[11] to be experimentally active for sacrificial water oxidation using a cobalt co-catalyst and a silver salt as SEA: the poly(dibenzothiophendioxide) homopolymer (P10, monomer J8, polymer 3240) and co-polymers of 1,4-dibromophenylene and 2,5-dibrompyridine (P24, monomers C6 and C7, polymer 1472) and 1,4-dibromophenylene and 2,5-dibromopyrazine (P28, monomers C6 and D1, polymer 1474). Conversely, the poly(p-phenylene) (P1, monomer C6, polymer 1471) and poly(thiophene) (P17, monomer C5, polymer 1411) homopolymers, which experimentally show no sign of water oxidation activity under the same conditions, are not included in the 30 or 50% because their IP values are predicted to be not sufficiently positive to oxidise water. The fact that our approach predicts polymers known to be active for sacrificial water oxidation to have IP values that are sufficiently positive to oxidise water, even when requiring an additional overpotential, and polymers known to be inactive to have IP values that are not sufficiently positive, gives us added confidence in our approach.

The fraction of polymers able to both reduce protons and oxidise water, for each overpotential value, increase steadily with pH. At pH 12.3, the same pH as for when using TEA as SED, we predict that approximately 70% of polymers straddle the proton reduction and water oxidation potentials and when requiring an additional 0.3 V

overpotential still more than 40% do so. These numbers are surprisingly similar to those discussed above for the case of where TEA instead of water is used as electron donor. Also, similar to when TEA is used as the SED, figures 3c and 3d show that if we require additionally for the polymer to have an optical gap small enough to absorb a large part of the visible spectrum relatively few polymers remain. Of the 3240 polymers in the dataset 3141 (96.9%) have an optical gap between 1.23 and 3.5 eV, 1128 (34.8%) have an optical gap between 1.23 and 2.5 eV and only 211 (6.5%) have an optical gap below 2 but above 1.23 eV (see dashed lines in figures 3b-3d). Moreover, just as for the case of the 1-electron oxidation of TEA and proton reduction, discussed above, only a fraction of those polymers with an optical gap between 1.23 and 2.5 eV and 1.23 and 2.0 eV will straddle the water splitting potentials. Even if all polymers with an optical gap between 1.23 and 2.5 eV or 1.23 and 2.0 eV would have an optical gap larger than 1.23 V, their IP and EA still might not straddle the water oxidation and proton reduction potentials because their IP is too deep or their EA to shallow. In contrast, polymers with a large optical gap will likely also have large fundamental gaps and thus will span the water splitting potentials for most realistic IP and EA values.
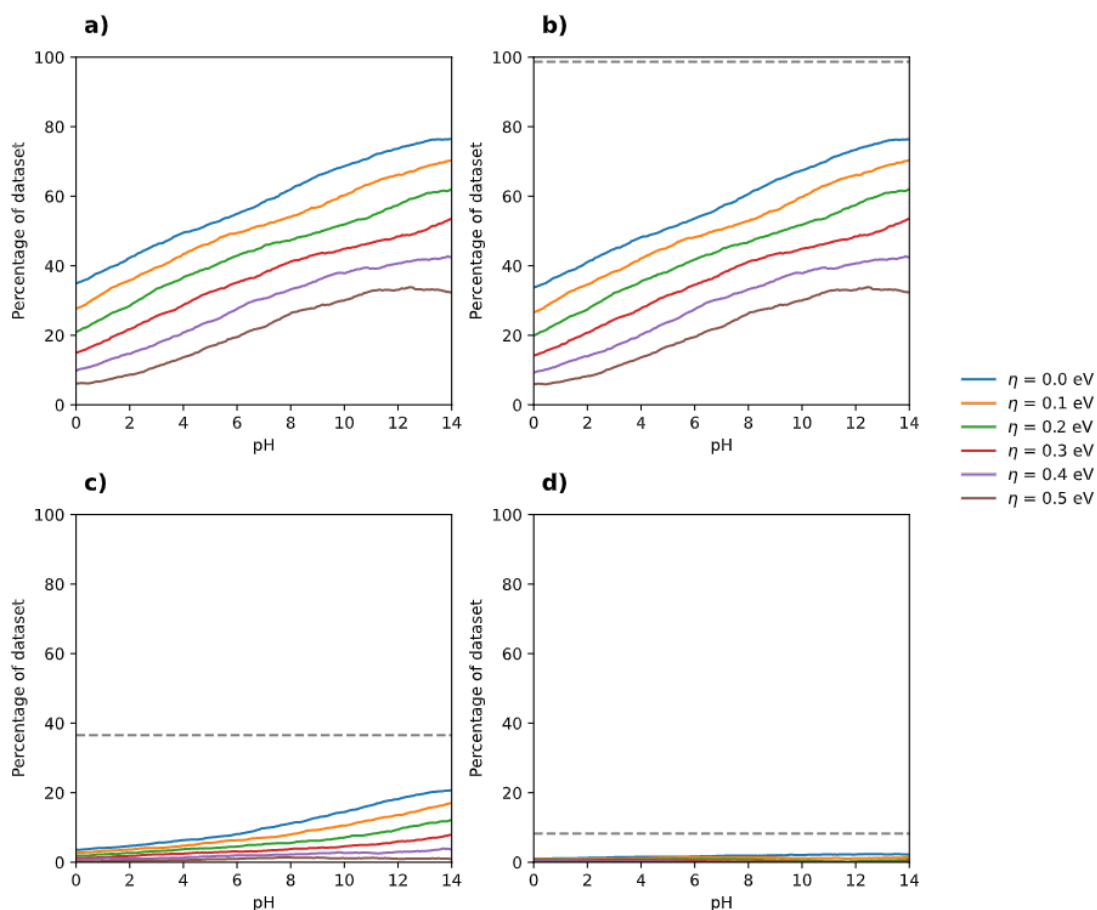
Fig. 3 *Percentage of (co-)polymers in the dataset that are predicted to be able to drive the overall splitting of water as a function of pH for different overpotential values and optical gap ranges. Panel (a) includes all polymers predicted to have an optical gap between 0.0 and 3.5 eV, panel (b) those with an optical gap between 1.23 eV and 3.5 eV f, panel (c) those with an optical gap between 1.23 eV and 2.5 eV, and 1.23 eV and 2.0 eV for panel (d). The grey dashed lines in panels b-d indicate the number of polymers in the entire dataset that fall within each optical gap constraint. See figure S3 for zoomed in version of a-d.*

The origin of the experimental scarcity of polymers that split water appears thus not to find its origin in any thermodynamic limitations of the material class. Many polymers are known to evolve hydrogen in the presence of TEA and very few to perform overall water splitting, even if in terms of thermodynamics similar numbers of polymers can drive both half-reaction pairs. We thus propose that the origin of the scarcity of polymer photocatalysts for overall water splitting is instead kinetic in nature. We previously[18] speculated this to be the case for specific polymers such as poly(pyridine)

based on calculations on poly(p-phenylene) and it. However, at that time it was computationally intractable to accurately calculate the properties for the large number of polymers required to perform adequate statistics, and thus demonstrate how common a property the thermodynamic ability to overall split water is for polymers, making the case for kinetics even stronger.

Overall TEA oxidation involves two electrons (holes) and water oxidation four, and while after the first electron transfer step TEA$^+$ likely diffuses away from the polymer, reducing the chance of the back electron transfer, the water oxidation intermediates probably stay adsorbed on co-catalyst surface until oxygen is formed, making back electron transfer more likely. Non-catalytic water oxidation by means of out-of-sphere electron transfer in analogy to the case of TEA is very unlikely because of the extreme potential of half-reaction associated with the initial one-hole oxidation of water (2.15 V at pH 7). In the case of a sluggish water-oxidation co-catalyst, electron-hole recombination hence likely outcompetes water oxidation. Similarly, sacrificial electron acceptors used in the case of sacrificial water oxidation, $e.g.,$ Ag$^+$ and Ce^{4+}, generally are thermodynamically easier to reduce than protons, i.e., have a more positive reduction potential, and only involve one rather than two electrons, meaning that in the presence of a sluggish water-oxidation co-catalyst, sacrificial water oxidation might be possible but overall water splitting not. The good news associated with this scenario is that this would mean that by choosing the right water oxidation co-catalyst a significant number of polymers should be active for overall water splitting. Indeed, experimentally the small number of polymers active for overall water splitting, were generally first reported to be only active for sacrificial water oxidation[8, 10] and only after optimisation of the water oxidation co-catalyst became active for overall water splitting.[13, 15] It would also suggest that combining polymers or polymers and small molecule acceptors together to make heterojunctions, splitting the excitons, and separating electrons and holes on separate sub-systems, reducing electron-hole recombination, should be a worthwhile strategy. As a matter of fact, bulk heterojunctions have been shown to yield promising results in the case of sacrificial hydrogen evolution.[46] Even in the presence of a heterojunction, however, the presence of efficient hydrogen and oxygen evolution co-catalysts is probably beneficial in terms

of the long-term stability of the polymer. Stability is not generally an issue in sacrificial hydrogen evolution with continuous hydrogen evolution for multiple days demonstrated for selected polymer materials without obvious signs of material degradation during this time.[21-23] However, the build-up of charges in the polymer,[47] especially holes, during overall water splitting in the presence of a sluggish water oxidation co-catalyst could result in material degradation and loss of activity. Reversely, a very active water oxidation co-catalyst, which very efficiently extracts charges from the polymer, might result in very stable polymer photocatalysts under overall water splitting conditions. For this reason, we also rule out that stability or lack thereof is the/a reason for the scarcity of overall water splitting photocatalysts.
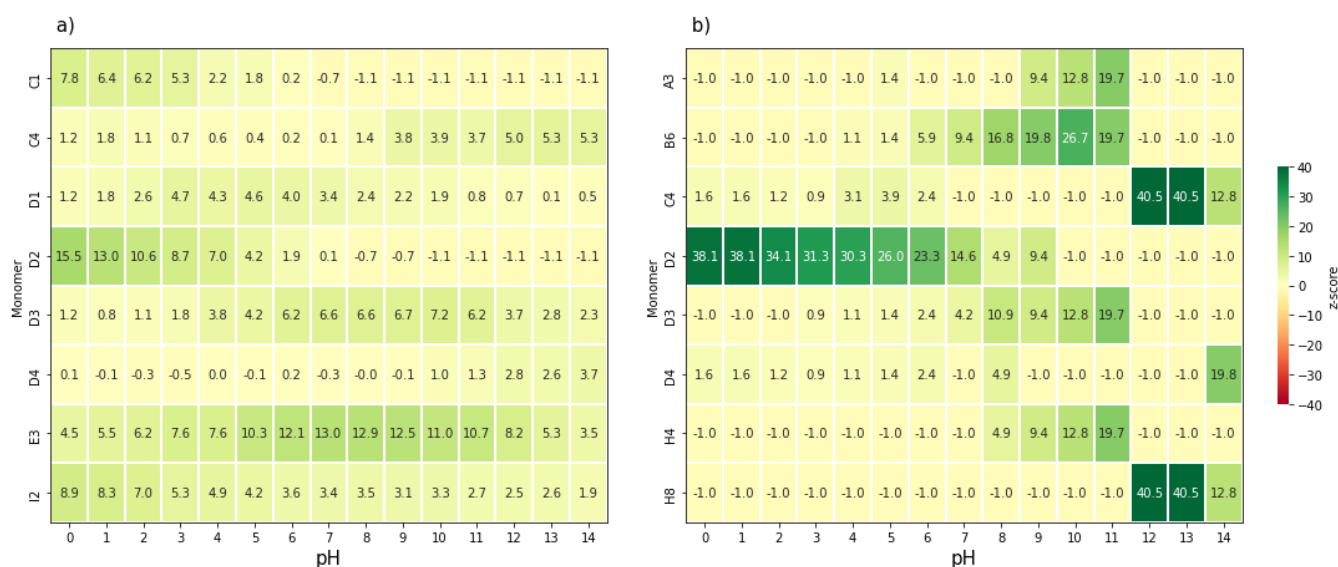

Fig. 4 *Heatmaps of the monomers with the highest z-score for watersplitting with overpotentials of 0.3 V, constrained by optical gap ranges (a) 1.23 - 2.5 eV and (b) 1.23 - 2.0 eV. The monomers which feature here correspond to those illustrated in figure 1c.*

One possible hurdle to efficient overall water splitting with polymer photocatalysts, even in the presence of optimal co-catalysts, is that relatively few (co-)polymers are, as discussed above, predicted to have the required driving force for proton reduction and water oxidation and absorb green to red light. However, it is important to stress here that such (co-)polymers are predicted to exist, discussed in more detail below, and this is not an issue unique to polymeric photocatalysts. As a matter of fact, many state-of-the-art inorganic solid-state photocatalysts, such as doped $SrTiO_3$, only absorb blue, violet and ultraviolet light[48-49] and developing systems that

are active on the red-side of the visible spectrum is also a challenge for inorganic materials.[48-49]

Finally, we analysed, by means of z-scores, which monomers are overrepresented under those binary AB co-polymers that can drive overall water splitting and absorb a large part of the visible spectrum. Figures 4a and 4b show the monomers with the highest z-score as a function of pH for polymers that can drive overall water splitting with an overpotential of 0.3 V and a predicted optical gap between 1.23 eV and 2.5 eV or 2.0 eV, respectively. At acidic pH, the monomer with the highest z-score for both optical gap ranges is 3,6-dibromo-1,2,4,5-tetrazine (D2, see figure 1C). This monomer occurs in 15 out of the 16 (< 2.0 eV) and 15 out of the 38 (< 2.5 eV) co-polymers that can drive overall water splitting at pH 0, respectively. For polymers with an optical gap below 2.5 eV several other monomers in the same neutral to acidic pH range also have relatively high z-scores: 1,4-dibromophthalazine (I2, occurring in 9 of the 38 co-polymers at pH 0) and 1,4-dibromo-2,3,5,6-tetranitrobenzene (C1, occurring in 8 of the 38 co-polymers at pH 0), see figure 4a. In contrast, as can be seen in figure 4b, no other monomers than D2 have high z-scores at acidic pH when we limit the optical gap to 2.0 eV. For D2, I2 and C1 the z-scores increase with decreasing pH, in line with the fact that these are all electron poor monomers that are likely to result in co-polymers with deep, very positive, IP values, and the fact that at low pH polymers are most likely limited by their ability to oxidise water. At high pH, for polymers with an optical gap below 2.0 eV, 2,5-dibromofuran (C4) and 5,8-dibromo-1,6-naphthyridine (H8), as well as 2,5-dibromo-2,5-dihydrofuro[3,2-*b*]furan (D4), have the highest z-scores, see figure 4b. At these pH values, > pH 12, water oxidation is thermodynamically easier relative to at low pH, explaining why some of these monomers are relatively electron rich (C4, D4). The overrepresentation of these monomers at alkaline pH values probably arises from the fact that co-polymers containing them have low(er) optical gaps rather than a deep IP. However, one should be careful not to overinterpret this data as the high z-scores in this region arise in part because very few polymers are predicted to have an optical gap < 2.0 eV and able to drive overall water splitting, specifically 6 polymers at pH 14, 3 of which contain D4 and 2 containing C4 or H8. For intermediate pH values between

neutral and alkaline, 4,7-dibromobenzo[*c*][1,2,5]oxadiazole (E3) has a relatively high z-score for polymers with an optical gap below 2.5 eV. E3 occurs in 35 out of 107 co-polymers with an optical gap < 2.5 eV that can drive overall water splitting at pH 7. 1,4-Dibromo-2,5-dinitrobenzene (B6), 2,5-dibromoaniline (A3), 2,5-dibromothiophene-1,1-dioxide (D3) and 1,4-dibromoisoquinoline (H4) have similarly high z-scores for polymers with an optical gap below 2.0 eV. Polymers based on all these monomers, other than 1,4-dibromo-2,3,5,6-tetranitrobenzene which is likely to be explosive and best avoided for that reason, should make good choices for future synthetic studies towards overall water splitting polymer photocatalysts. This is especially true of monomers like D2 and E3 for which a large number of polymers are predicted to be able to drive overall water splitting and have a small optical gap: 15 out of the 80 (co-)polymers in the data-set containing D2 (19%) are predicted to have an optical gap < 2.0 eV and able to drive overall water splitting at acid pH while 35 out the 80 (co-)polymers containing E3 in the data-set (44%) are predicted to have an optical gap < 2.5 eV and able to drive overall water splitting at neutral pH. Leads in term of co-monomers in the case of D2 at acidic pH include 3,7-dibromodibenzo[*b,d*]thiophene-5,5-dioxide (J8), 2,5-dibromopyrazine (D1), 2,5-dibromopyrimidine (C8), 2,7-dibromo-9*H*-fluoren-9-one (J5), 2,5-dibromoterephthalonitrile (B2), 1,4-dibromo-2,5-bis(trifluoromethyl)benzene (B7), 1,4-dibromo-2-nitrobenzene (A8) and E3. Similarly, co-monomer leads for E3 at neutral pH include A8, B2, B7, C8, D1, 1,4-dibromo-2-fluorobenzene (A2), 1,4-dibromo-2,5-difluorobenzene (A6), 1,4-dibromo-2,3,5,6-tetrafluorobenzene (B4), 2,5-dibromobenzonitrile (A4), 1,4-dibromo-2-(trifluoromethyl)benzene (B1), 2,5-dibromopyridine (C7) and most nitrogen substituted naphtalenes (e.g. E6 and F2).

Conclusions

Thermodynamically a significant number of conjugated polymers are predicted to be able to drive overall water splitting, a similar number as polymers able to drive hydrogen evolution when oxidising triethylamine as a sacrificial electron donor. As many polymers are known experimentally to evolve hydrogen in the presence of triethylamine, we argue that the scarcity of polymers performing overall water splitting is not due to any thermodynamic constraints but rather probably has a kinetic origin,

with overall water splitting requiring an efficient co-catalyst for the water oxidation. Moreover, in the presence of such co-catalysts, it is likely that a significant number of polymers that are very active for sacrificial hydrogen evolution, will also be active for overall water splitting. Considering the rapid development of polymer photocatalysts and increase in sacrificial hydrogen production rates we believe that now more effort must be made to study water oxidation with polymer photocatalysts, focusing on developing suitable co-catalysts, given that this is currently a bottleneck in developing systems for overall water splitting and our work suggests that this is a realistic target. A large hurdle for efficient overall water splitting with visible light, finally, is found to be the fact that only a relatively small number of the co-polymers studied are predicted to absorb yellow to red light. However, this is similarly an issue for inorganic photocatalysts, with many state-of-the-art inorganic photocatalysts, e.g. $SrTiO_3$, only absorbing blue, violet and ultraviolet light.

Author Contributions

BS performed the calculations and analysed the results. BS, LW and MAZ conceived the study. LW assisted in the z-score calculations. AWP assisted in the thermodynamic analysis and RSS provided a synthetic perspective. MAZ supervised the work. All authors contributed to the writing of the manuscript and have approved the final version.

Conflicts of Interest

There are no conflicts to declare.

Supplementary Information

Electronic supplementary information (ESI) available: SMILES representation and pictures of all monomers, calibration parameters used and predicted IP, EA and optical gap for all (co-)polymers.

Acknowledgements

References

1.   Vyas, V. S.; Lau, V. W.-h.; Lotsch, B. V., Soft Photocatalysis: Organic Polymers for Solar Fuel Production. *Chemistry of Materials* **2016**, *28*, 5191-5204.

2.   Wang, Y.; Vogel, A.; Sachs, M.; Sprick, R. S.; Wilbraham, L.; Moniz, S. J. A.; Godin, R.; Zwijnenburg, M. A.; Durrant, J. R.; Cooper, A. I.; Tang, J., Current Understanding and Challenges of Solar-Driven Hydrogen Generation Using Polymeric Photocatalysts. *Nature Energy* **2019**, *4*, 746-760.

3.   Kosco, J.; Moruzzi, F.; Willner, B.; McCulloch, I., Photocatalysts Based on Organic Semiconductors with Tunable Energy Levels for Solar Fuel Applications. *Advanced Energy Materials* **2020**, *10*, 2001935.

4.   Banerjee, T.; Podjaski, F.; Kröger, J.; Biswal, B. P.; Lotsch, B. V., Polymer Photocatalysts for Solar-to-Chemical Energy Conversion. *Nature Reviews Materials* **2021**, *6*, 168-190.

5.   Bai, Y.; Hippalgaonkar, K.; Sprick, R. S., Organic Materials as Photocatalysts for Water Splitting. *Journal of Materials Chemistry A* **2021**, *9*, 16222-16232.

6.   Bai, Y.; Wilbraham, L.; Slater, B. J.; Zwijnenburg, M. A.; Sprick, R. S.; Cooper, A. I., Accelerated Discovery of Organic Polymer Photocatalysts for Hydrogen Evolution from Water through the Integration of Experiment and Theory. *Journal of the American Chemical Society* **2019**, *141*, 9063-9071.

7.   Meier, C. B.; Clowes, R.; Berardo, E.; Jelfs, K. E.; Zwijnenburg, M. A.; Sprick, R. S.; Cooper, A. I., Structurally Diverse Covalent Triazine-Based Framework Materials for Photocatalytic Hydrogen Evolution from Water. *Chemistry of Materials* **2019**, *31*, 8830-8838.

8.   Wang, X.; Maeda, K.; Thomas, A.; Takanabe, K.; Xin, G.; Carlsson, J. M.; Domen, K.; Antonietti, M., A Metal-Free Polymeric Photocatalyst for Hydrogen Production from Water under Visible light. *Nature Materials* **2009**, *8*, 76-80.

9.   Bi, J.; Fang, W.; Li, L.; Wang, J.; Liang, S.; He, Y.; Liu, M.; Wu, L., Covalent Triazine-Based Frameworks as Visible Light Photocatalysts for the Splitting of Water. *Macromolecular Rapid Communications* **2015**, *36*, 1799-1805.

10.   Lan, Z.-A.; Fang, Y.; Zhang, Y.; Wang, X., Photocatalytic Oxygen Evolution from Functional Triazine-Based Polymers with Tunable Band Structures. *Angewandte Chemie International Edition* **2018**, *57*, 470-474.

11.   Sprick, R. S.; Chen, Z.; Cowan, A. J.; Bai, Y.; Aitchison, C. M.; Fang, Y.; Zwijnenburg, M. A.; Cooper, A. I.; Wang, X., Water Oxidation with Cobalt-Loaded Linear Conjugated Polymer Photocatalysts. *Angewandte Chemie International Edition* **2020**, *59*, 18695-18700.

12.   Liu, J.; Liu, Y.; Liu, N.; Han, Y.; Zhang, X.; Huang, H.; Lifshitz, Y.; Lee, S.-T.; Zhong, J.; Kang, Z., Metal-Free Efficient Photocatalyst for Stable Visible Water Splitting Via a Two-Electron Pathway. *Science* **2015**, *347*, 970-974.

13.   Zhang, G.; Lan, Z.-A.; Lin, L.; Lin, S.; Wang, X., Overall Water Splitting by Pt/G-C$_3$N$_4$ Photocatalysts without Using Sacrificial Agents. *Chemical Science* **2016**, *7*, 3062-3066.

14.	Kong, D.; Han, X.; Xie, J.; Ruan, Q.; Windle, C. D.; Gadipelli, S.; Shen, K.; Bai, Z.; Guo, Z.; Tang, J., Tunable Covalent Triazine-Based Frameworks (CTF-0) for Visible-Light-Driven Hydrogen and Oxygen Generation from Water Splitting. *ACS Catalysis* **2019**, *9*, 7697-7707.

15.	Zhang, S.; Cheng, G.; Guo, L.; Wang, N.; Tan, B.; Jin, S., Strong-Base-Assisted Synthesis of a Crystalline Covalent Triazine Framework with High Hydrophilicity Via Benzylamine Monomer for Photocatalytic Water Splitting. *Angewandte Chemie International Edition* **2020**, *59*, 6007-6014.

16.	Pan, Z.; Liu, M.; Zhang, G.; Zhuzhang, H.; Wang, X., Molecular Triazine–Heptazine Junctions Promoting Exciton Dissociation for Overall Water Splitting with Visible Light. *The Journal of Physical Chemistry C* **2021**, *125*, 9818-9826.

17.	Guiglion, P.; Butchosa, C.; Zwijnenburg, M. A., Polymer Photocatalysts for Water Splitting: Insights from Computational Modeling. *Macromolecular Chemistry and Physics* **2016**, *217*, 344-353.

18.	Guiglion, P.; Butchosa, C.; Zwijnenburg, M. A., Polymeric Watersplitting Photocatalysts; a Computational Perspective on the Water Oxidation Conundrum. *Journal of Materials Chemistry A* **2014**, *2*, 11996-12004.

19.	Prentice, A. W.; Zwijnenburg, M. A., The Role of Computational Chemistry in Discovering and Understanding Organic Photocatalysts for Renewable Fuel Synthesis. *Advanced Energy Materials* **2021**, *11*, 2100709.

20.	Guiglion, P.; Monti, A.; Zwijnenburg, M. A., Validating a Density Functional Theory Approach for Predicting the Redox Potentials Associated with Charge Carriers and Excitons in Polymeric Photocatalysts. *The Journal of Physical Chemistry C* **2017**, *121*, 1498-1506.

21.	Woods, D. J.; Hillman, S. A. J.; Pearce, D.; Wilbraham, L.; Flagg, L. Q.; Duffy, W.; McCulloch, I.; Durrant, J. R.; Guilbert, A. A. Y.; Zwijnenburg, M. A.; Sprick, R. S.; Nelson, J.; Cooper, A. I., Side-Chain Tuning in Conjugated Polymer Photocatalysts for Improved Hydrogen Production from Water. *Energy & Environmental Science* **2020**, *13*, 1843-1855.

22.	Sprick, R. S.; Bonillo, B.; Clowes, R.; Guiglion, P.; Brownbill, N. J.; Slater, B. J.; Blanc, F.; Zwijnenburg, M. A.; Adams, D. J.; Cooper, A. I., Visible-Light-Driven Hydrogen Evolution Using Planarized Conjugated Polymer Photocatalysts. *Angewandte Chemie International Edition* **2016**, *55*, 1792-1796.

23.	Sachs, M.; Sprick, R. S.; Pearce, D.; Hillman, S. A. J.; Monti, A.; Guilbert, A. A. Y.; Brownbill, N. J.; Dimitrov, S.; Shi, X.; Blanc, F.; Zwijnenburg, M. A.; Nelson, J.; Durrant, J. R.; Cooper, A. I., Understanding Structure-Activity Relationships in Linear Polymer Photocatalysts for Hydrogen Evolution. *Nature Communications* **2018**, *9*, 4968.

24.	Sprick, R. S.; Aitchison, Catherine M.; Berardo, E.; Turcani, L.; Wilbraham, L.; Alston, B. M.; Jelfs, K. E.; Zwijnenburg, M. A.; Cooper, A. I., Maximising the Hydrogen Evolution Activity in Organic Photocatalysts by Co-Polymerisation. *Journal of Materials Chemistry A* **2018**, *6*, 11994-12003.

25.	Sprick, R. S.; Wilbraham, L.; Bai, Y.; Guiglion, P.; Monti, A.; Clowes, R.; Cooper, A. I.; Zwijnenburg, M. A., Nitrogen Containing Linear Poly(Phenylene) Derivatives for Photo-Catalytic Hydrogen Evolution from Water. *Chemistry of Materials* **2018**, *30*, 5733-5742.

26.	Bannwarth, C.; Caldeweyher, E.; Ehlert, S.; Hansen, A.; Pracht, P.; Seibert, J.; Spicher, S.; Grimme, S., Extended Tight-Binding Quantum Chemistry Methods. *WIREs Computational Molecular Science* **2021**, *11*, e1493.

27.	Wilbraham, L.; Berardo, E.; Turcani, L.; Jelfs, K. E.; Zwijnenburg, M. A., High-Throughput Screening Approach for the Optoelectronic Properties of Conjugated Polymers. *Journal of Chemical Information and Modeling* **2018**, *58*, 2450-2459.

28. Heath-Apostolopoulos, I.; Wilbraham, L.; Zwijnenburg, M. A., Computational High-Throughput Screening of Polymeric Photocatalysts: Exploring the Effect of Composition, Sequence Isomerism and Conformational Degrees of Freedom. *Faraday Discussions* **2019**, *215*, 98-110.

29. Wilbraham, L.; Smajli, D.; Heath-Apostolopoulos, I.; Zwijnenburg, M. A., Mapping the Optoelectronic Property Space of Small Aromatic Molecules. *Communications Chemistry* **2020**, *3*, 14.

30. Heath-Apostolopoulos, I.; Vargas-Ortiz, D.; Wilbraham, L.; Jelfs, K. E.; Zwijnenburg, M. A., Using High-Throughput Virtual Screening to Explore the Optoelectronic Property Space of Organic Dyes; Finding Diketopyrrolopyrrole Dyes for Dye-Sensitized Water Splitting and Solar Cells. *Sustainable Energy & Fuels* **2021**, *5*, 704-719.

31. Grimme, S.; Bannwarth, C.; Shushkov, P., A Robust and Accurate Tight-Binding Quantum Chemical Method for Structures, Vibrational Frequencies, and Noncovalent Interactions of Large Molecular Systems Parametrized for All SPD-Block Elements (Z = 1–86). *Journal of Chemical Theory and Computation* **2017**, *13*, 1989-2009.

32. Ásgeirsson, V.; Bauer, C. A.; Grimme, S., Quantum Chemical Calculation of Electron Ionization Mass Spectra for General Organic and Inorganic Molecules. *Chemical Science* **2017**, *8*, 4879-4895.

33. Grimme, S.; Bannwarth, C., Ultra-Fast Computation of Electronic Spectra for Large Systems by Tight-Binding Based Simplified Tamm-Dancoff Approximation (sTDA-xTB). *The Journal of Chemical Physics* **2016**, *145*, 054103.

34. Turcani, L.; Berardo, E.; Jelfs, K. E., STK: A Python Toolkit for Supramolecular Assembly. *Journal of Computational Chemistry* **2018**, *39*, 1931-1942.

35. *https://github.com/lukasturcani/stk*.

36. Riniker, S.; Landrum, G. A., Better Informed Distance Geometry: Using What We Know to Improve Conformation Generation. *Journal of Chemical Information and Modeling* **2015**, *55*, 2562-2574.

37. *https://www.rdkit.org/*.

38. Halgren, T. A., Merck Molecular Force Field. I. Basis, Form, Scope, Parameterization, and Performance of MMFF94. *Journal of Computational Chemistry* **1996**, *17*, 490-519.

39. *https://github.com/grimme-lab/xtb*.

40. Onufriev, A. V.; Case, D. A., Generalized Born Implicit Solvent Models for Biomolecules. *Annual Review of Biophysics* **2019**, *48*, 275-296.

41. *https://github.com/LiamWilbraham/molz*.

42. Bai, Y.; Wilbraham, L.; Gao, H.; Clowes, R.; Yang, H.; Zwijnenburg, M. A.; Cooper, A. I.; Sprick, R. S., Photocatalytic Polymers of Intrinsic Microporosity for Hydrogen Production from Water. *Journal of Materials Chemistry A* **2021**, *9*, 19958-19964.

43. Kosco, J.; Sachs, M.; Godin, R.; Kirkus, M.; Francas, L.; Bidwell, M.; Qureshi, M.; Anjum, D.; Durrant, J. R.; McCulloch, I., The Effect of Residual Palladium Catalyst Contamination on the Photocatalytic Hydrogen Evolution Activity of Conjugated Polymers. *Advanced Energy Materials* **2018**, *8*, 1802181.

44. Sachs, M.; Cha, H.; Kosco, J.; Aitchison, C. M.; Francàs, L.; Corby, S.; Chiang, C.-L.; Wilson, A. A.; Godin, R.; Fahey-Williams, A.; Cooper, A. I.; Sprick, R. S.; McCulloch, I.; Durrant, J. R., Tracking Charge Transfer to Residual Metal Clusters in Conjugated Polymers for Photocatalytic Hydrogen Evolution. *Journal of the American Chemical Society* **2020**, *142*, 14574-14587.

45.	Prentice, Andrew W.; Zwijnenburg, M. A., Hydrogen Evolution by Polymer Photocatalysts; a Possible Photocatalytic Cycle. *Sustainable Energy & Fuels* **2021**, *5*, 2622-2632.

46.	Kosco, J.; Bidwell, M.; Cha, H.; Martin, T.; Howells, C. T.; Sachs, M.; Anjum, D. H.; Gonzalez Lopez, S.; Zou, L.; Wadsworth, A.; Zhang, W.; Zhang, L.; Tellam, J.; Sougrat, R.; Laquai, F.; DeLongchamp, D. M.; Durrant, J. R.; McCulloch, I., Enhanced Photocatalytic Hydrogen Evolution from Organic Semiconductor Heterojunction Nanoparticles. *Nature Materials* **2020**, *19*, 559-565.

47.	Sekar, A.; Sivula, K., Organic Semiconductors as Photoanodes for Solar-Driven Photoelectrochemical Fuel Production. *CHIMIA International Journal for Chemistry* **2021**, *75*, 169-179.

48.	Wang, Q.; Domen, K., Particulate Photocatalysts for Light-Driven Water Splitting: Mechanisms, Challenges, and Design Strategies. *Chemical Reviews* **2020**, *120*, 919-985.

49.	Chen, S.; Takata, T.; Domen, K., Particulate Photocatalysts for Overall Water Splitting. *Nature Reviews Materials* **2017**, *2*, 17050.